Functional role of Kv1.3 localization in chimeric antigen receptor T cells

Ghofrane Medyouni, Orsolya Vörös, György Panyi, Péter Hajdu

The Journal of Immunology, 2025, **214**, 2796–2805
https://doi.org/10.1093/jimmun/vkaf199
Advance access publication August 24, 2025
Research Article

American Association of Immunologists™

OXFORD

Functional role of Kv1.3 localization in chimeric antigen receptor T cells

Ghofrane Medyouni[1], Orsolya Vörös[1], György Panyi[1], and Péter Hajdu[1,2,*]

[1]Department of Biophysics and Cell Biology, Faculty of Medicine, University of Debrecen, Debrecen, Hungary
[2]Division of Dental Biochemistry, Faculty of Dentistry, University of Debrecen, Debrecen, Hungary

*Corresponding author: Department of Biophysics and Cell Biology, Faculty of Medicine, University of Debrecen, Egyetem tér 1, Debrecen H-4032, Hungary. Email: hajdup@med.unideb.hu.

Abstract

Chimeric antigen receptor (CAR) T-cell therapy has proven to be a promising treatment for multiple types of cancer. Yet, the mechanisms regulating CAR T-cell function as well as the side effects remain an area of active research. The formation of the immunological synapse is essential for the activation of signaling pathways including the Ca^{2+}-dependent one. Here we demonstrated the functional role of Kv1.3 channels in a CAR T-cell model. Our findings highlight the colocalization of Kv1.3 channel with CAR and its redistribution into the synapse between a CAR T and target cell. The biophysical properties of Kv1.3 channel are not vastly affected by the introduction of CAR in the cells. The blockage of this ion channel's lateral movement affects the killing potential of CAR T cells, likely via disruption of the Ca^{2+} response upon IS formation. Overall, these data suggest that the manipulation of the Kv1.3 channel may contribute to the improvement of CAR T-cell immunotherapy and provide new insights for future clinical strategies.

Keywords: cancer, CAR T cell, CRAC, immunotherapy, Kv1.3

Introduction

Ion channels plunged into the world of immunology more than 40 years ago once it became releasable to record electrical signals from single cells of the immune system. A key component in the immune system is the T cells.[1] Along with the several intracellular pathways involved in the regulation of their function, it became clear that ion channels actively contribute to cellular functions including proliferation, migration, and cytokine release such as IL-2, IL-4, IL-17, IFN-γ, and TNF.[2] In addition to other channels, Kv1.3, KCa3.1, and CRAC channels are involved in this functional network.[1] Several studies showed this; eg Chirra and colleagues conducted a comprehensive review and analysis on the impact of K^+ channel activity on T-cell survival, cytokine production, and motility.[3] The expression levels of these ion channels in human T lymphocytes depend on the cell state of differentiation.[1] At rest, T cells express lower levels of these channels. However, upon antigen binding, $CCR7^+$ naive and central memory T cells upregulate KCa3.1 whereas $CCR7^-$ upregulates Kv1.3. In the activation state, the driving force for the Ca^{2+} entry via CRAC channels is maintained by the membrane potential, which is adjusted mainly by Kv1.3 and KCa3.1. After antigen binding, IP3 binds to its receptor, which causes the release of Ca^{2+} from the store followed by the activation of the CRAC channels. The Ca^{2+} influx activates the calcineurin-NFAT pathway leading to gene transcription.[4,5] The changes in the cytosolic Ca^{2+} concentration, especially in the immune synapse, are important for the cell lysis function of $CD8^+$ cytotoxic T cells.[6] Recent studies revealed that regulating these channels leads to a better outcome in terms of killing efficiency. It has been shown for example, that blocking KCa3.1 increases the killing efficiency of a subpopulation of human NK lymphocytes.[7] As for migration, other studies proved that a defect in KCa3.1 limits the ability of $CD8^+$ T cells of cancer patients to infiltrate the tumor microenvironment (TME). The importance of these potassium channels of T cells has been also verified in cancer in mice models where the overexpression of Kv1.3 increased the IFN-γ production and reduced tumor and survival.[8,9]

Over the past few years, the development of genetically engineered T cells with chimeric antigen receptors (CARs) has launched a new area for immunotherapy. CAR recognizes a specific tumor antigen in a non-MHC-restricted manner and activates pathways leading to T-cell activation.[10] A CAR T-cell therapy approved by the U.S. Food and Drug Administration was successfully applied to treat blood cancer patients in recent years.[11] The design of CARs has undergone much upgrading, resulting in different generations achieving a higher efficacy. Despite its clinical success, several treated patients suffer from severe side effects such as cytokine release syndrome and neurotoxicity. Furthermore, this approach still faces many limitations, eg the treatment of solid tumors due to the heterogeneity of these tumors. On the other hand, CAR-T cells might not be able to infiltrate the tumors because of the less-expressed chemokines in tumor tissues.[12] Moreover, the TME is rich in suppressor cells such as myeloid-derived suppressor cells and regulatory T cells. This can heavily alter the activity of CAR T cells. Most tumors are described as rich in adenosine and reactive oxygen species. These agents disrupt T cell responses.[13] Previous research highlighted the effect of KCa3.1 channels in the adenosine-mediated suppression of the migration of $CD8^+$ T cells and suggested that it can be a therapeutic tool to increase the ability to infiltrate the adenosine-rich TME.[14]

Little is known about the role of ion channels in CART cells. We published before that CAR expression alters ion

Received: March 14, 2025. **Accepted:** July 8, 2025

channel expression in T cells and that these channels' modifications can alter target cell elimination by these cells. A better understanding of CAR T cell physiology could help to establish a novel generation of genetically modified T cells that have the desired activities aiding to target solid tumors, persist, and act under the harsh TME conditions. Hence, in the present study we used a T-cell line to generate CAR T cells, and studied the role and membrane distribution of Kv1.3 channels in standalone and target cell–engaged CAR T cells. We also evaluated the effect of channel localization on the function of the CAR T cells.

Materials and methods

Cell culture and retroviral transduction

HEK-293T cells were cultured in DMEM (Sigma-Aldrich, Hungary) that contained 10% FBS, 1 mM Na-pyruvate, 2mM GlutaMAX and 200 units of penicillin-streptomycin. Cells were maintained at 37 °C in a humidified atmosphere of 5% CO_2 and 95% air. Cells were passed every 2 days.

Before transfection, 2×10^6 cells of HEK293T cells was plated in a 10-cm plate with 10 mL of DMEM supplemented with 10% FBS. To proceed, the cells were required to adhere to the plate and reach 70% confluence. First, 4 μg of pBMN–sGFP–CAR (sGFP: superfolding green fluorescent protein) or pBMN-empty vector (for backbone plasmid info see https://www.addgene.org/1734/, CAR: 3rd generation anti-CD19 CAR see ref[15]), 3 μg of psPAX2 (plasmid info: https://www.addgene.org/12260/), and 3 μg of VSV.G (plasmid info: https://www.addgene.org/14888/) were mixed and diluted in 500 μL of jetPRIME buffer, followed by the addition of 20 μL of jetPRIME reagent (Polyplus, Illkirch, France) with subsequent incubation for 10 min at room temperature. As a last step, the transfection mixture was added to the plate containing the cells in the medium and incubated for 48 h. The sGFP signal was used as a reporter on the transfection of the HEK293T cells with pBMN-sGFP-CAR; therefore, cells were checked under the microscope for GFP positivity. The viral supernatant was removed from the HEK293T cells and collected, filtered using a 0.45-μM filter, then added to the target Jurkat cells, along with the polybrene (10 μg/mL). Following 48 h of incubation at 37 °C in a humidified atmosphere of 5% CO_2 and 95% air, transduced cells were centrifuged and cultured in a T25 flask with fresh medium. The transduction efficacy was checked with flow cytometry using nontransduced (NT) Jurkat cells as a control for the cells transduced with pBMN-sGFP-CAR. As for the cells transduced with the empty vector of pBMN, the antibiotic selection marker was utilized to select these cells.

Cell sorting

As the transduction efficiency was at most 74%, to culture only the sGFP-positive (CAR-expressing) cells, we used a cytoFLEX flow cytometer to sort the cells. At first, 1×10^6 of the transduced cells was centrifuged and washed with PBS, then resuspended in 1% FBS-PBS. Jurkat-NT cells were used as a negative control. After sorting, cells were centrifuged for 5 min, $300 \times g$ at room temperature (RT), then re-suspended in RPMI medium and placed in the incubator to grow at 37 °C in a humidified environment of 5% CO_2/95% air, with the RPMI medium replenished every 2 or 3 d. Results were analyzed with FCS Express 6 software.

Patch-clamp technique

Jurkat-NT, Jurkat-CAR (Jurkat cell expressing pBMN-sGFP-CAR), and Jurkat-PBMN (Jurkat cell expressing pBMN-empty) cells were washed with the standard extracellular solution (composition was in mM: 145 NaCl, 5 KCl, 1 $MgCl_2$, 2.5 $CaCl_2$, 5.5 glucose, 10 HEPES, pH 7.35), and plated onto cell culture 35-mm petri dishes. Kv1.3 currents were recorded in whole-cell configuration using an Axopatch 200B amplifier (Molecular Devices, Sunnyvale, CA, USA). The intracellular solution consisted of (in mM): 140 KF, 11 K_2 EGTA, 1 $CaCl_2$, 2 $MgCl_2$, and 10 HEPES (pH 7.20, ∼295 mOsm).

The activation kinetics of the current were characterized by fitting the Hodgkin–Huxley model ($I[t] = I_a \times (1 - \exp[-t/\tau_a])^4 + C$, where I_a is the amplitude of the activating current component; τ_a is the activation time constant of the current; and C is the current at the beginning of the trace) to the rising phase of the current trace obtained by 15-ms-long depolarization to +50 mV. The activation time constant characterizes the average of the time constants of a given cell upon 3 sequential depolarizations repeated every 15 s.

The inactivation kinetics of the current were characterized by fitting a single exponential function ($I[t] = I_0 \times \exp(-t/\tau_{in}) + C$, where I_0 is the amplitude of the current, τ_{in} is the inactivation time constant, and C is the steady-state value of whole-cell current at the end of the pulse) to the decaying part of the current traces obtained by 2-s-long depolarization to +40 mV from a holding potential of −120 mV. The inactivation time constant was determined as for the activation, except that pulses were delivered every 60 s.

The voltage dependence of steady-state activation was determined as follows: Jurkat-NT, Jurkat-CAR, and Jurkat-PBMN cells were held at −120 mV holding potential and depolarized to various test potentials ranging from −70 mV to +50 mV in 10-mV steps at every 30 s. Peak whole-cell conductance [G(V)] at each test potential was calculated from the peak current (I_p) at test potential V and the K^+ reversal potential ($E_r = -85$ mV) using $G(V) = I_p/(V - E_r)$. The G(V) values were normalized for the maximum conductance and plotted as a function of test potential and the Boltzmann function was fitted to the data points: $G_N = 1/(1 + \exp[-(V - V_{1/2})/k])$, where G_N is the normalized conductance, V is the test potential, $V_{1/2}$ is the midpoint or half-maximal activation potential, and k is the slope factor of the function.

Calcium imaging

To investigate the effect of CAR expression on the CRAC-related Ca^{2+} response, a FURA-2 Ca^{2+} imaging technique was applied. At first, Jurkat-CAR/NT/PBMN cells were plated in poly-L-lysine–coated glass-bottom petri dishes, then loaded with 1 μM FURA 2-acetoxymethyl ester (Thermo Fisher Scientific, Budapest, Hungary) dissolved in DMSO and incubated for 30 min at 37 °C in phenol red–free RPMI solution (Sigma-Aldrich), supplemented with 1% FBS, 2 mM L-glutamine, 1 mM Na-pyruvate, and 200 units penicillin-streptomycin.

Afterward, we washed the cells with 2 mM Ca^{2+} solution (143.3 mM NaCl, 4.7 mM KCl, 10 mM HEPES, 5.5 mM glucose, 2 mM $CaCl_2$, 1 mM $MgCl_2$, pH 7.35) and placed them on a 37 °C stage of an inverted fluorescence microscope. Later on, the Jurkat-CAR cells were perfused with 2 mM Ca^{2+}solution, 0 mM Ca^{2+}, 143.3 mM NaCl, 4.7 mM KCl, 10 mM HEPES, 5.5 mM glucose, 1 mM $MgCl_2$, 0.1 mM EGTA, pH 7.35), and then 1 μM thapsigargin (TG) (Thermo

Fisher Scientific) containing 0 mM Ca^{2+} solution was applied to deplete the Ca^{2+} stores via passive release from the endoplasmic reticulum. After store depletion, the addition of the extracellular 2 mM Ca^{2+} containing 1 μM TG activated intracellular Ca^{2+} elevation through store-operated calcium entry (SOCE). Experiments with FURA-2 were done with an inverted Nikon ECLIPSE Ts2R microscope combined with a VisiChrome High-Speed Polychromator (Visitron Systems GmbH, Puchheim, Germany). FURA-2 dual excitation and emission were accomplished using 340 nm and 380 nm excitation filters and a 510 nm emission filter. Digital images (200 ms exposure) were recorded with a PCO Edge 4.2 sCMOS camera at 10-s intervals. Data acquisition and analyses were accomplished using VisiView 4.0.0.11 imaging software. Only GFP-positive cells were selected for Jurkat-CAR cells.

CAR and Kv1.3 colocalization

Jurkat-CAR cells were plated onto poly-L-lysine coverslips for 30 min at 37 °C (2×10^5 cells/coverslip) in a humidified chamber and then washed 3 times with PBS at room temperature. Cells were fixed with 1% formaldehyde for 10 min at room temperature. For blocking unspecific binding, we added 20% FBS in PBS to the cells for 30 min at room temperature. To stain the Kv1.3, we used the anti-Kv1.3 (KCNA3) extracellular antibody (Alomone Labs) rabbit IgG at 1:50 concentration in 10% FBS-PBS overnight at 4 °C. Next, cells were washed with PBS and the secondary antibody Alexa Fluor 647 goat anti-rabbit was added at 1:800 in PBS for 45 min on ice in the dark. Coverslips were washed 3 times with PBS and then mounted onto slides with Fluromount G. Images were taken with Nikon N–STORM confocal microscope. Based on the fluorescent spectrum of the GFP and Alexa Fluor 647, laser lines 488 and 647 nm were used to detect the signal. Recorded images were analyzed with Image J software using the Colocalization 2 plugin.

Immunological synapse formation

To investigate the immunological synapse (later we refer to it as CAR synapse) between the Jurkat-CAR and the Raji cells, the synapse was formed at a ratio of 1:1. First the cells were mixed and co-centrifuged for 1 min, at 37 °C, 200 × *g*. The mix was dropped on poly-L-lysine–treated coverslips and incubated for 60 min at 37 °C. Then, cells were fixed with 4% formaldehyde for 10 min, washed 3 times with PBS, and blocked with 20% FBS-PBS for 45 min. Then Kv1.3 channels were labeled as detailed at colocalization, and the next day cells were permeabilized with 0.1% TritonX-100, and blocking was performed with 20% BSA-PBS for 45 min at RT. Cells were washed 3 times with PBS and labeled with the primary antibody of CD19 (HIB19 by BioLegend) in 10% BSA-PBS and incubated at 4 °C overnight. Afterward, cells were washed again with PBS 3 times, and anti-mouse Alexa Fluor 647 IgG was added (1:1,000, 45 min, RT). Finally, the cells were washed with PBS, and coverslips were mounted onto microscopy slides using Fluoromount-G. The samples were examined by the confocal microscope Nikon N-STORM, with the excitation lasers set to 488, 561, and 647 nm, and the images were analyzed by Image J software. To evaluate the Kv1.3 accumulation ratio, we used the method described previously.[16]

Calcein Red-AM–based killing assay

To test the killing potential of our CAR cells, we performed a Calcein Red-AM–based killing assay. First, Raji cells (target cells) were stained with Calcein Red-AM. Then, 3×10^6 cells was centrifuged for 5 min at 300 × *g* and resuspended in PBS, and 1 μM of the dye was used to stain the cells for 30 min at 37 °C. Cells were plated into an 8-well Ibidi chamber in phenol red–free RPMI with 1% FBS. In the co-cultures the ratio was 1:2 (effector : target). Then cells were incubated for 3 h in a humidified cell culture incubator at 37 °C. Recorded images were analyzed with Image J software using the ROI tool to measure the Calcein Red-AM intensity.

Calcium imaging in CAR synapse

Immune synapse was performed between Raji and Jurkat-CAR/NT cells. For staining the target cells, we used the CMTPX cell tracker (Thermo Fisher, C34552). Then, 1×10^6 of Raji cells was centrifuged for 5 min at 300 × *g* and 1 μM of CMTPX was added in serum-free culture medium. Cells were incubated for 30 min at 37 °C in the dark. Afterward, cells were washed 2 times and resuspended in phenol red–free medium RPMI with 10% FBS. The labeled Raji cells were plated in the petri dish with the Jurkat CAR at a ratio of 1:1.

The Ca^{2+} response with FURA-2 was recorded as described above except that the images were recorded every 30 s for 1 h without a change in the solutions or application of TG. The recording starting time point is at the moment of adding the Raji cells. The same experiment was also performed with crosslinking the Kv1.3 and with adding only a secondary antibody (IgG isotype) as described below. Only engaged cells were analyzed.

Kv1.3 crosslinking

Kv1.3 channels were immobilized by antibody complexes of rabbit anti-Kv1.3 antibody and anti-rabbit goat IgG. First, Jurkat-CAR cells were incubated on ice for 1 h with polyclonal anti-Kv1.3 antibody against an extracellular epitope at a 100:1 ratio of antibody:Kv1.3 α subunit (0.8 μg antibody/10 mL cell suspension of 2 million cells/mL). This concentration was determined considering, on average, the expression of ca. 400 Kv1.3 channels/cell and the fact that each channel is formed by 4 α-subunits. The incubation with Kv1.3 antibody was followed by a 30-min incubation with anti-rabbit IgG. Control cells underwent the same experimental steps with adding an isotype IgG (referred as Ab2 condition).

Results

Generation of Jurkat CAR anti-CD19 model

In this study, we used a third-generation CD19-CAR model targeting the CD19 molecule on the B-cell surface. Our construct is composed of CD19 single–chain variable fragment, CD8 as a transmembrane domain, CD28, 4-1BB, and CD3z sGFP in the cytosolic part.[15] A Jurkat T-cell line stably expressing this CD19-CAR construct (Jurkat-CAR) was established through retroviral transduction followed by FACS of sGFP-positive, ie CAR-presenting cells (Fig. 1A, 95% of cells were $sGFP^+$). To test the functionality of this model, we proceeded with a Calcein Red-AM–based killing assay adopted from Kummerow et al.[17] Calcein Red-AM is a cell-permeant fluorescent probe. The signal intensity of the Calcein Red is proportional to the cell vitality. The increase in the nonspecific membrane permeability of target cells, here

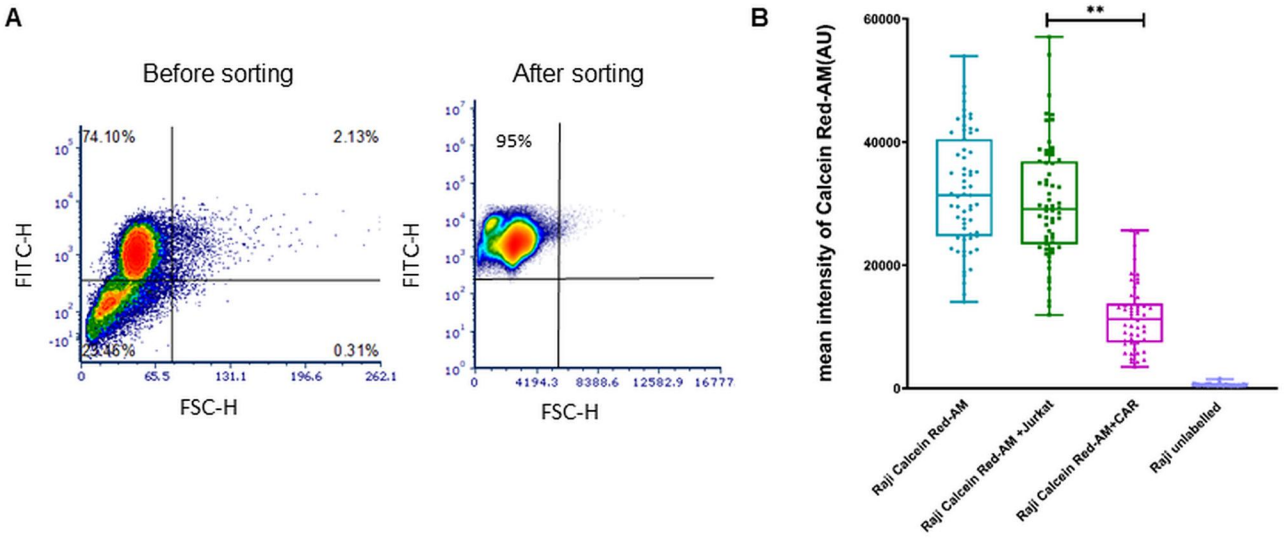

Figure 1. Generation and validation of CAR T-cell line. (A) Left: sGFP-FSC density plot of the CD19-CAR transduced Jurkat cells. Here 74% of cells were sGFP positive. sGFP was detected in the FITC channel. Right: Dotplot (FSC vs sGFP) of sorted Jurkat-CAR cells showed 95% positivity. (B) Calcein Red-AM–based killing assay for Jurkat-CAR cells and NT-Jurkat cells. Boxplot of Calcein Red intensity values; each symbol represents the mean intensity of Calcein Red for a cell. Raji Calcein Red-AM: Raji B cells loaded with dye, no effector cells added; Raji Calcein Red-AM + Jurkat: dye-loaded Raji cells incubated with NT-Jurkat cells; Raji Calcein Red-AM + CAR: dye-loaded Raji cells incubated with Jurkat-CAR cells; Raji unlabeled: unstained Raji cells. The E:T ratio is 1:1; measurements were performed on 3 different days, $n \geq 30$. $^{**}P < 0.01$.

we used $CD19^+$ Raji B-cell line as a target cell, leads to efflux of the dye and indicates the irreversible phase of cell death. The results of the killing assay shown in Fig. 1B reveal that the intensity of Calcein Red dropped when Raji cells were co-cultured for 3 h with Jurkat-CAR cells, unlike for NT-Jurkat cells, suggesting that Jurkat-CAR cells specifically eliminate the target cells even within this short period. Therefore, the generated CAR-expressing model cell line could be applied in the subsequent experiments related to the ion channel, specifically Kv1.3.

The presence of CAR slightly shifts the voltage dependence of steady-state activation for Kv1.3

Next, we sought to determine whether the introduction of CAR into the Jurkat T-cell line can change the properties of the voltage-gated potassium channel Kv1.3, which contributes to the Ca^{2+}-activated pathway in T cells. Current of Kv1.3 channels in Jurkat-CAR, NT-Jurkat, and Jurkat-PBMN cells were analyzed to learn the biophysical parameters of the channel. As shown in Fig. 2A and B, the activation and inactivation kinetics were the same in Jurkat-CAR cells compared to NT-Jurkat and Jurkat-PBMN cells (τ_a for NT-Jurkat is 0.65 ± 0.04 ms, for Jurkat-PBMN is 0.64 ± 0.04 ms, for Jurkat-CAR is 0.85 ± 0.08 ms; τ_i for NT-Jurkat is 201.3 ± 21 ms, for Jurkat-PBMN is 168.2 ± 11.4 ms, for Jurkat-CAR is 220.4 ± 20 ms). We also assessed the equilibrium parameters of membrane potential dependence of activation: The test-potential vs normalized conductance curves show that the slope factor (k) is the same for Jurkat-CAR/NT-Jurkat and Jurkat-CAR/Jurkat-PBMN (slope: NT-Jurkat: 9.84 ± 0.6 mV, Jurkat-CAR: 10.95 ± 0.6 mV, Jurkat-PBMN: 13.80 ± 1 mV; $P > 0.05$, Fig. 2C). The half-maximal voltage ($V_{1/2}$) was higher for the Jurkat-CAR cells than NT-Jurkat cells (V_{half} for NT-Jurkat: -29.24 ± 3.2 mV, Jurkat-CAR: -20.37 ± 1.9 mV) as indicated by the rightward shift of the steady-state activation curve. The comparison of the half-maximal voltage between NT-Jurkat/Jurkat-PBMN and Jurkat-CAR/Jurkat-PBMN cells was nonsignificant (V_{half} for Jurkat-PBMN: -23.43 ± 1 mV; $P > 0.05$). These data demonstrate that the Kv1.3 steady-state activation is slightly affected by the presence of the CAR receptor in the plasma membrane and suggests that it could be partially linked to the viral transduction itself. Motivated by these findings, we next performed a Ca^{2+} imaging measurement to get an insight into this pathway.

Jurkat-CAR has a lowered TG-induced Ca^{2+} response

It was reported previously that Ca^{2+} is a key factor for T-cell effector function. A recent study found that cytotoxic T cells and NK cells require an optimum intracellular Ca^{2+} level for efficient cancer cell elimination.[18] To learn the functional expression of CRAC channels, we performed a FURA-2–based Ca^{2+} imaging experiments. Upon the stimulation with TG and readdition of the 2 mM extracellular Ca^{2+} even in the presence of TG, the cytosolic Ca^{2+} increase could be observed, which is due to the influx of Ca^{2+} through the pore formed by CRAC channels. The control NT-Jurkat and Jurkat-PBMN cells had a typical Ca^{2+} response as shown in Fig. 3A, while the representative trace of the cytosolic Ca^{2+} level (average of 20 to 30 cells) displays that Jurkat-CAR cells had a significantly lower CRAC-related response, ie the SOCE is lowered. The ratio of intensity ratios detected in the presence of 2 mM Ca^{2+} over the baseline (0 mM Ca^{2+} solution with TG, just before addition of 2 mM Ca^{2+}) was significantly higher in NT-Jurkat compared to Jurkat-CAR cells (Fig. 3B; $P = 0.009$) and also significantly different between Jurkat-PBMN and Jurkat-CAR cells ($P = 0.01$). These data clearly demonstrate that TG-induced Ca^{2+} response is attributed to the CAR expression and not to the retroviral transduction of cells.

Kv1.3 channel is colocalized with the CAR receptor and present in the immune synapse

The immune synapse (IS) is a dynamic cellular interaction between the target cell and the effector cell. Previous studies

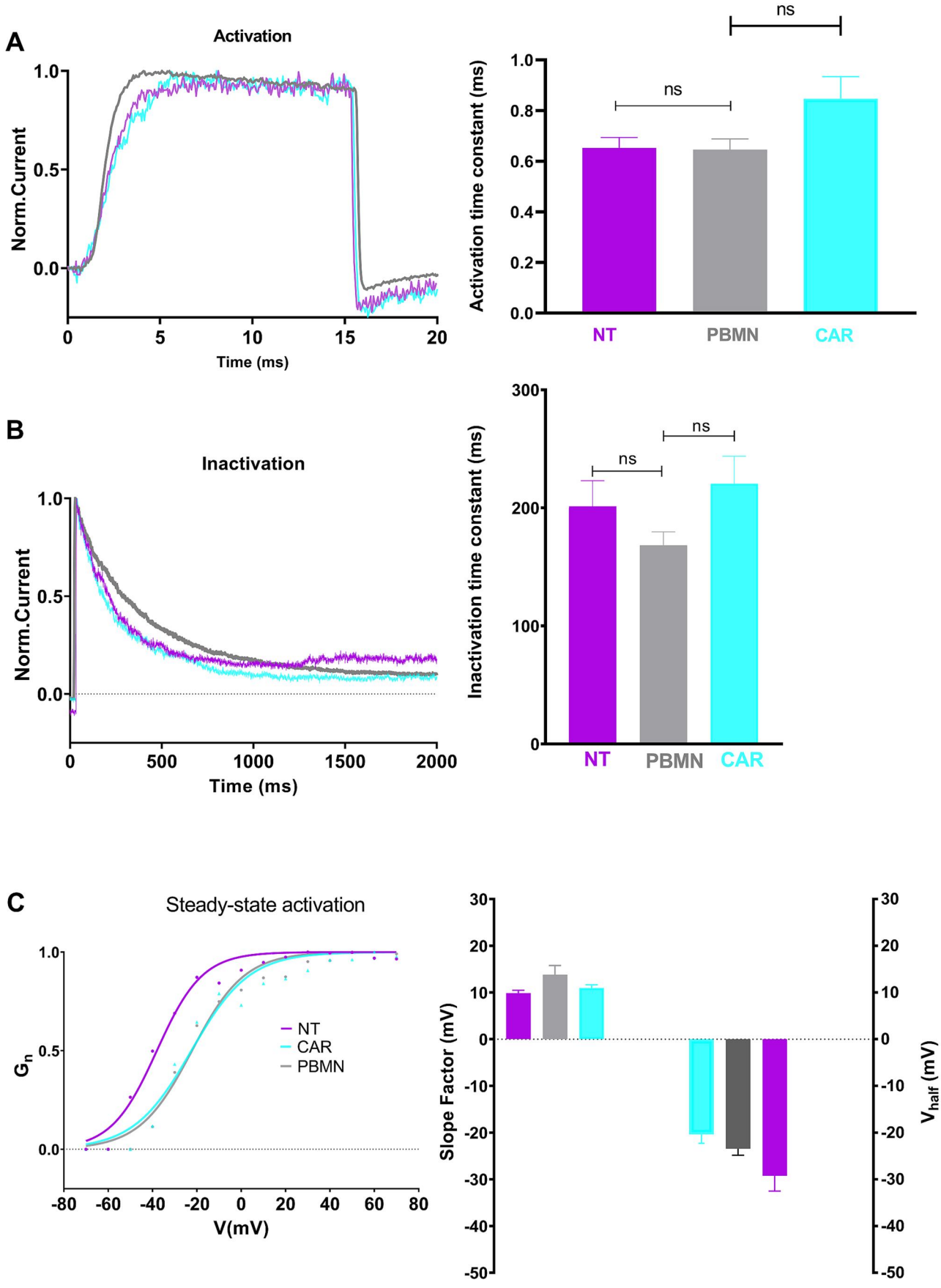

Figure 2. Biophysical properties of Kv1.3 channel in Jurkat-CAR cells. (A) Activation kinetics. Left: Current traces of an NT-Jurkat, Jurkat-CAR, Jurkat-PBMN cell recorded upon 15-ms-long, +50 mV depolarization, holding was −120 mV. Right: Kv1.3 current activation time constant of Jurkat-CAR, NT-Jurkat, and Jurkat-PBMN cells. (B) Inactivation kinetics. Left: Current traces recorded upon depolarization to +40 mV for 2 s from −120 mV holding potential. Right: inactivation time constant for Kv1.3 current in Jurkat-CAR, NT-Jurkat, and Jurkat-PBMN cells. (C) Voltage dependence of steady-state activation. Left: The test potential vs normalized conductance along with the best-fit Boltzmann curves for a Jurkat-CAR, NT-Jurkat, and Jurkat-PBMN cell. Right: The equilibrium parameters' activation, $V_{1/2}$, and the slope factor (k), $n = 3$ to 8, ns: not significant.

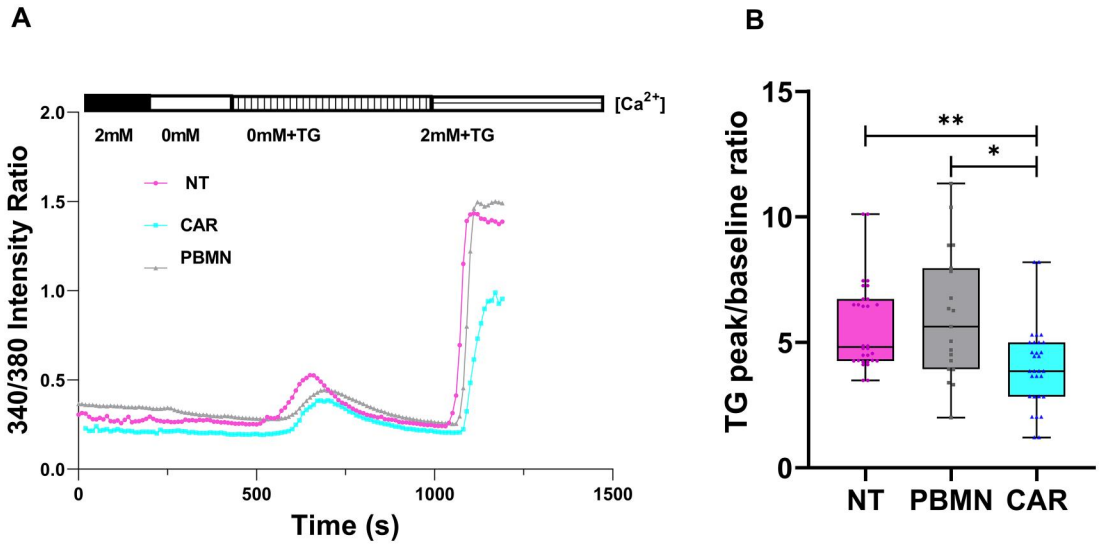

Figure 3. Cytosolic Ca^{2+} measurements using FURA-2 in Jurkat-CAR, NT-Jurkat, and Jurkat-PBMN cells. (A) Cytosolic Ca^{2+} representative traces of Jurkat-CAR (blue), Jurkat-NT (pink), and Jurkat-PBMN (gray) cells on the 340 nm/380 nm intensity ratio. For the representative traces, at least 30 cells were recorded. (B) Boxplot of baseline Ca^{2+} intensity ratios for Jurkat-CAR (blue), Jurkat-NT (pink), and Jurkat-PBMN (gray) cells. Each point represents a single-cell value, $n = 20$ to 30. $^{*}P < 0.05$, $^{**}P < 0.01$.

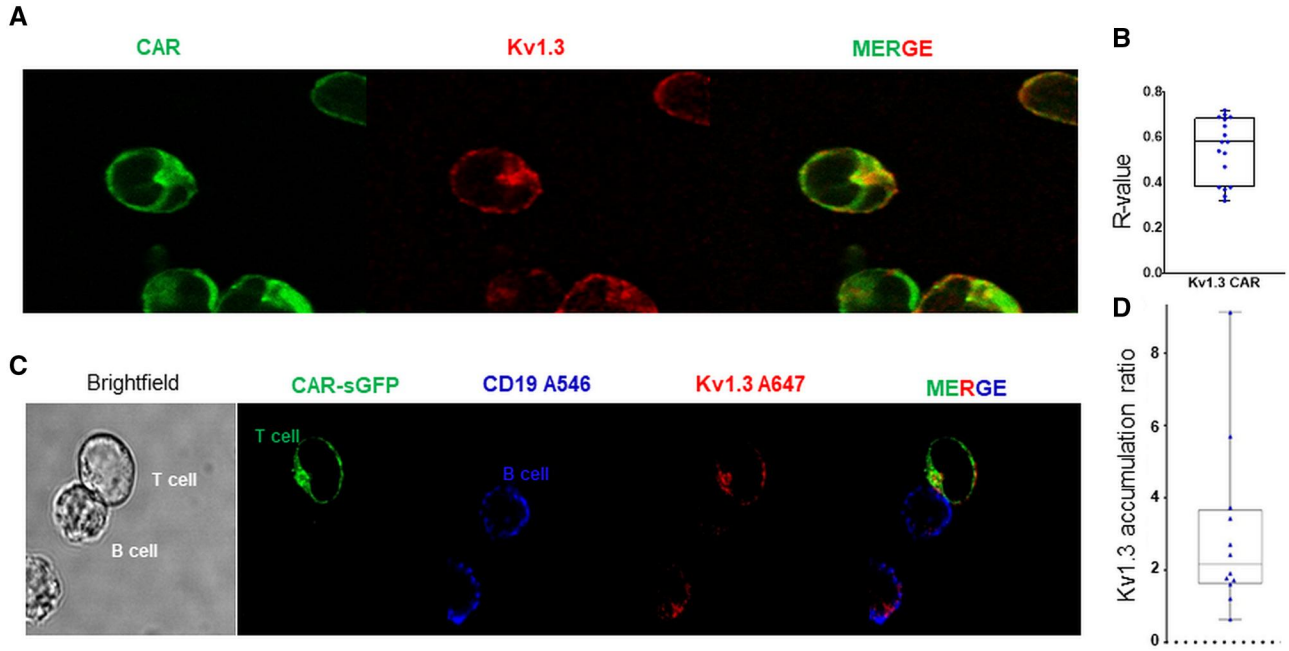

Figure 4. Co-localization of CAR and Kv1.3 in Jurkat-CAR cells and Kv1.3 accumulation in the immunological synapse between Jurkat-CAR and Raji cells. (A) Confocal images of Jurkat-CAR cells stained with anti-Kv1.3 antibody (second antibody is goat anti-rabbit IgG with Alexa Fluor 647). Left: CAR with sGFP (green), middle: Kv1.3 with Alexa Fluor 647 (red), right: merge of green and red channels. (B) Dotplot of Pearson coefficients for colocalization of CAR and Kv1.3, $n = 17$. (C) Confocal images of immune synapse formed between a CAR (green) cell and a Raji (blue) cell. Kv1.3 was stained with rabbit anti-Kv1.3 and goat anti-rabbit Alexa Fluor 647, and Raji cells were stained with mouse anti-CD19 and goat anti-mouse Alexa Fluor 546; the merge of the channels (blue and red) shows the accumulation of Kv1.3 in the CAR synapse. (D) Boxplot of Kv1.3 accumulation ratio observed in the synapse after 60 min.

pointed out that Kv1.3 channels redistribute into the IS and revealed the possibility of regulating the activity of this channel to control the signaling initiated in the IS.[19] For that reason, we studied the localization of CARs and Kv1.3 channels in standalone (colocalization) and IS-engaged (Kv1.3 redistribution) Jurkat-CAR cells. Confocal images of Jurkat-CAR cells labeled with Kv1.3 antibody are shown in Fig. 4A: the patchy fluorescence of Kv1.3 channels and sGFP signal of CAR show high overlapping regions. Using Image J software, we analyzed the colocalization of Kv1.3 and CAR and found that the Pearson correlation coefficient (mean of *R*-value is 0.53 ± 0.04), which indicates the proximity of these 2 proteins in the cell membrane (Fig. 4B).

No study reported before about the presence of the Kv1.3 channel in the immunological synapse formed between a CAR T cell and a target Raji B cell (we refer to this synapse as CAR synapse or CS to differ from CD3/MHC-related immune synapse). We therefore generated CS between Jurkat-

CAR cells and Raji cells and assessed the rearrangement of Kv1.3 channels into the contact region between the effector and the target cells (Fig. 4C). To confirm the CS formation, we monitored the CAR accumulation in the contact area of the 2 cells.[15] Fig. 4D shows that Kv1.3 of Jurkat-CAR cells redistributes to the CS, which is further confirmed by the accumulation ratio value (2.99 ± 0.6; $P = 0.001$) displayed in Fig. 4D. The importance of Kv1.3 in the synaptic regions was described before: It alters the Ca^{2+}-dependent signaling pathway and may result in hyperactivity of T cells.[20]

The inhibition of the Kv1.3 recruitment to the synapse abolishes target cell elimination of Jurkat-CAR cells

The functional implication of Kv1.3 in this CS between Jurkat-CAR cells and Raji cells is still unknown. Previously, our results showed that blocking the Kv1.3 with the specific blocker Vm24 facilitates the killing potential of CAR T cells.[21] Here, we wanted to learn if blocking of Kv1.3 relocation to the synapse influences the CAR cells canonical function, namely target cell elimination. As before, we tested the killing capacity of Jurkat-CAR cells: We hindered the Kv1.3 channels' CS accumulation with antibody crosslinking as previously described[20] and then co-incubated these cells with Raji target cells. Fig. 5 displays that the immobilization of Kv1.3 channels suppressed the Jurkat-CAR cells' target cell elimination ability compared to the control cells (Raji + Jurkat-CAR cells) and to the only second antibody-treated (Ab2 condition) cells (Raji + Jurkat-CAR cells + second antibody). These findings demonstrate that the hampering of Kv1.3 channels' membrane redistribution to the CS in Jurkat-CAR cells affects the efficiency of target elimination.

Ca^{2+} response of Jurkat-CAR cells is Kv1.3 location dependent

It was previously reported that the Kv1.3 channel redistribution and accumulation in the immune synapse is involved in the shaping Ca^{2+} signaling.[20] Other studies reported that immune synapse residency of ion channels (Orai1/CRAC and Kv1.3) influence the Ca^{2+} response of T cells.[16,22] Hence, we carried out Ca^{2+} imaging measurements upon forming a CS between a Jurkat-CAR and a Raji cell to investigate the effect of preventing the trafficking of Kv1.3 into the synapse. These experiments were designed to evaluate the Ca^{2+} response of NT-Jurkat cells, Jurkat-CAR cells, Jurkat-CAR cells with crosslinked Kv1.3, and Jurkat-CAR cells in the presence of the isotype IgG (secondary antibody), referred to as the Ab2 condition.

Upon engaging with the target cell, 100% of NT-Jurkat cells showed, as we presumed, no change in the baseline Ca^{2+} level and it remained the same throughout the whole recording period (60 min, Fig. 6D). However, Jurkat-CAR cells possessed different response in Ca^{2+} level upon coming in contact with a Raji cell: (1) The majority (47%) of cells had an oscillatory response up to the end of the recording period (Fig. 6A); (2) fewer cells (30%) display oscillatory Ca^{2+} levels with declining baseline (Fig. 6B); (3) few showed (23%) multiple lone Ca^{2+} spikes without oscillation (Fig. 6C, E). In the case of Jurkat-CAR cells in the presence of Ab2, calcium responses were similar to that observed as for its absence (Fig. 6E). Just as for NT-Jurkat cells, the Kv1.3 trafficking-restricted Jurkat-CAR cells (Kv1.3 was crosslinked before FURA-2 loading) did not respond with any change in the intracellular Ca^{2+} level upon engagement with a Raji cell (Fig. 6D). These differences seen in Ca^{2+} signaling could be related to differences in downstream signaling pathways, highlighting the importance of the Kv1.3 relocation in the initiation of cell death machinery. It may be due to the fact of the differences in immunoreceptor tyrosine-based activation motifs between the TCR and CAR initiating the phosphorylation cascade.

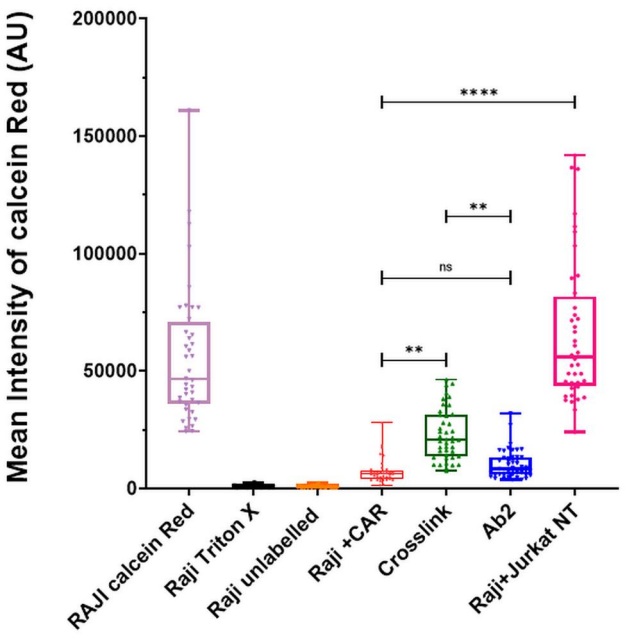

Figure 5. Kv1.3 immobilization suppresses target cell elimination. Boxplot of Calcein Red intensity values; each symbol represents the mean intensity of Calcein Red for a cell. Raji Calcein Red-AM: Raji B cells loaded with dye, no effector cells added; Raji + Triton X; Raji Calcein Red-AM + Jurkat: dye-loaded Raji cells incubated with NT-Jurkat cells; Raji Calcein Red-AM + CAR: dye-loaded Raji cells incubated with Jurkat-CAR cells; Raji unlabeled: unstained Raji cells; Raji Calcein Red-AM + CAR with crosslinking Kv1.3; Raji Calcein Red-AM + CAR with secondary antibody only. Kv1.3 channels were crosslinked using a ratio of 100:1 of antibody Kv1.3 α subunit, the E:T ratio is 1:2, and measurements were performed on 3 different days. $^{**}P < 0.01$, $^{****}P < 0.0001$.

Discussion

CAR T-cell immunotherapy still faces many challenges to be overcome. Even though this therapy has been the cure for several patients suffering from mostly nonsolid tumors, it was shown that the side effects are life-threatening.[23] The need for a better understanding of this genetically engineered T cells is crucial to regulate its function. Though targeting ion channels is typical in several diseases (multiple sclerosis, Parkinson disease, psoriasis, epilepsy, etc), little is known about their role in CAR T-cell therapy.[24] Previous studies already highlighted the leading role that K^+ channels in the Ca^{2+}-activated pathways.[25]

In current study, we designed a CD19-recognizing third-generation CAR T-cell model using a Jurkat cell line, which was reported previously as an adequate approach for characterization of CAR in T cells.[26] Using whole-cell patch-clamp technique, we unveiled the biophysical properties of the Kv1.3 channel upon CAR expression. Our results show a minor shift in the steady-state activation curve toward depolarizing potentials (rightward) in Jurkat-CAR cells, which likely has an impact on Ca^{2+} signaling. Motivated by this, we

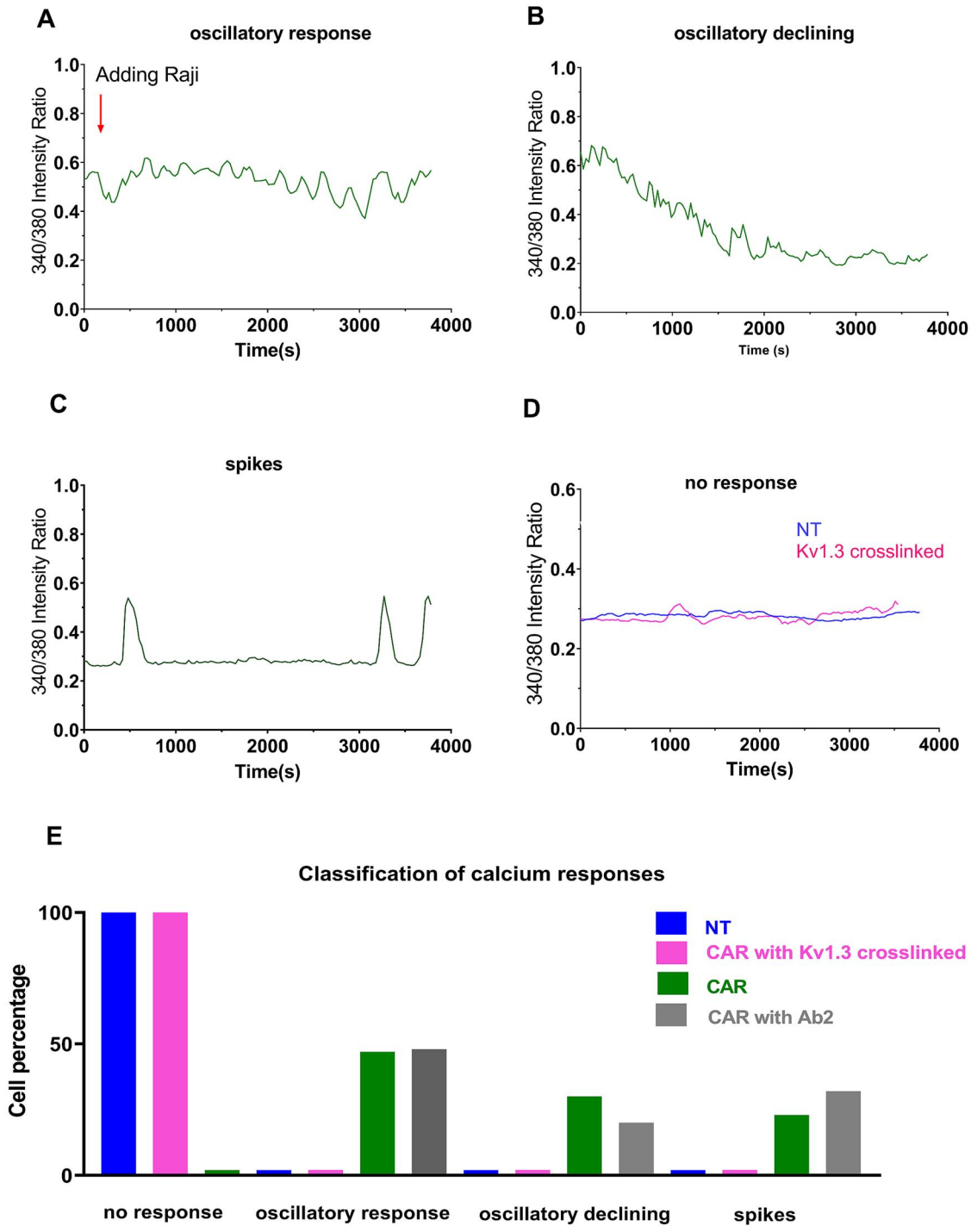

Figure 6. Ca^{2+} response of Jurkat-CAR cells diminishes in the lack of Kv1.3 CAR synapse accumulation. Representative traces of cytosolic FURA-2–based Ca^{2+} measurements in Jurkat-CAR cells: (A) oscillatory response with steady baseline, (B) oscillatory with declining baseline, (C) multiple, lone spikes. (D) Response of NT-Jurkat and Jurkat-CAR cells upon crosslinking Kv1.3 in a synapse with a Raji CD19 cell. The arrow indicates the addition of Raji target cells. (E) Classification of Ca^{2+} response in NT-Jurkat cells, Jurkat-CAR cells, Kv1.3-crosslinked Jurkat-CAR cells, and Jurkat-CAR cells incubated with second antibody only (Ab2). $n \geq 30$.

evaluated the Ca^{2+} response of Jurkat-CAR cells: The CRAC-dependent Ca^{2+} amplitudes were hampered in comparison to the NT-Jurkat and Jurkat-PBMN cells (Fig. 3A). Previously, we also described this phenomenon in CAR T cells; hence, we suppose that introducing CAR can modify the expression of proteins shaping TG-induced Ca^{2+} uptake. Alternatively, the change in the Kv1.3 activation can lead to a lower Ca^{2+} level. However, the optimal intracellular Ca^{2+} level could be different for various functions; hence, this decrease could be beneficial for the killing potential of Jurkat-CAR cells.

Here, we could show the colocalization of the Kv1.3 with the CAR receptor, which assumes a functional coupling between the CAR and the channel. Furthermore, the accumulation of CAR cells along with Kv1.3 channels in the synapse between Jurkat-CAR and Raji cells was demonstrated.

It was reported previously that the localization and persistence of Kv1.3 channels of T cells in the immunological synapse modulated the Ca^{2+} response,[20] which probably causes the hyperactivity of T cells. Also, the colocalization of Kv1.3 with CD3 was described in T cells, the proximity of which could also have functional relevance as suggested in a previous report[27]; however, CD3 and Kv1.3 (exogenous) reside in different IS region in CD4 cells.

To learn how the Kv1.3 synapse redistribution affects effector functions, we prevented Kv1.3 channel IS trafficking in Jurkat-CAR cells as described before.[20] The crosslinking experiment clearly showed that the recruitment of the Kv1.3 channel is important for the good performance of Jurkat-CAR cells: Blocking of Kv1.3 synapse redistribution partially suppressed the killing potential. We suppose this could be explained with the following: (1) Not all Jurkat cells express Kv1.3, so these cells are still able to induce the cell death in target cells; (2) as Kv1.3 and CAR are probably present in the same membrane domain, Kv1.3 immobilization interferes with CAR relocation to the synaptic region; consequently, no encounter formation with target cells occurs; and (3) the Ca^{2+}-dependent pathway is not exclusive in the target cell elimination. The first could be excluded, as using patch-clamp we observed the presence of Kv1.3 current almost in every Jurkat-CAR cell. The second is also not probable, as the number of CAR cells far exceeds the number of Kv1.3 channels in Jurkat-CAR cells (Fig. 4), and we also showed that the CAR "polarization" was the same at 60 min for control and crosslinked cells (Fig. S1). We think there is an ample number of CAR cells, which can migrate to the synapse and initiate cell death in target cells. Probably, the Kv1.3 and Ca^{2+} influx–independent activation via CD28 and 4-1BB could underline this not black-or-white situation.

On the other hand, previously we showed that blocking conductivity of Kv1.3 channels with a specific blocker could lead to enhanced killing rate in CAR T cells manufactured from primary $CD8^+$ T cells (24-h vs 3-h assay here), which also express KCa3.1, the other channel necessary for Ca^{2+}-dependent functions.[21] However, Jurkat cells do not have KCa3.1, which could compensate for the missing Kv1.3 function in T cells; hence, the target cell killing could be hampered, at least in the early phase/short period.[28,29]

To unveil how crosslinking of Kv1.3 channels affects the Ca^{2+}-dependent pathway, we tested the Ca^{2+} response in Jurkat-CAR cells. When NT-Jurkat cells monitored upon Raji–target cell binding, no Ca^{2+} signal was observed throughout a long period (up to 60 min), which clearly shows the specificity of CAR–CD19 interaction. However, the Ca^{2+} signaling of Jurkat-CAR cells (and Jurkat-CAR cells incubated with only secondary antibody [Ab2 condition], Fig. 6E) was remarkably different: The periodic/oscillatory changes in Ca^{2+} level went on up to the 60th min. Previously, we reported that Jurkat cells' Ca^{2+} response could be characterized with a single-peak response, with a few oscillations for a short period of time, when these cells were provoked via the CD3/TCR complex.[16] A difference in TCR- and CAR-induced Ca^{2+} signaling was also reported before; however, the flow cytometric analysis performed here does not allow for an appropriate comparison.[30] Crosslinking of Kv1.3 completely abolished the Ca^{2+}-level changes upon Jurkat-CAR–Raji encounter formation. Nicolaou et al described before that Ca^{2+} signaling is also affected by the Kv1.3 IS-localization, but in their experiments, T cells were triggered via the CD3/CD28 pathway.[22] Hence, we can conclude that Kv1.3 modulation could be a target in achieving better therapeutic outcome.

Here we reported that Kv1.3 channels' synapse redistribution affects the effector function of Jurkat-CAR T cells. We must mention that there are some limitations to this study such as studying the signaling pathways, which seems to be more complicated since it was reported that TCR and CAR do not stimulate the same signaling pathways.[31] However, we suggest that the results presented could direct further studies in order to better comprehend and develop this therapy.

Acknowledgments

The authors thank Cecilia Nagy and Adrienn Bagosi for their technical assistance, Xiaolei Su (Yale University, New Haven, CT, USA) for the plasmid used to generate the CAR model, and Hegedüs Éva for the pBMN-empty vector (University of Debrecen).

Author contributions

Ghofrane Medyouni (Conceptualization [lead], Data curation [lead], Formal analysis [lead], Funding acquisition [lead], Investigation [lead], Methodology [lead], Writing—original draft [lead]), Orsolya Vörös (Formal analysis [supporting], Methodology [supporting]), György Panyi (Conceptualization [supporting], Supervision [supporting], Validation [supporting]), and Péter Hajdu (Conceptualization [lead], Formal analysis [lead], Investigation [lead], Methodology [lead], Supervision [lead], Writing—review & editing [lead])

Supplementary material

Supplementary material is available at *The Journal of Immunology* online.

Funding

This research was funded by the NRDIO/NKFIH (National Research, Development and Innovation Office) K128525, University of Debrecen Program for Scientific Publication; the University of Debrecen Scientific Research Bridging Fund (DETKA) (to P.H.); and the Stipendium Hungaricum Scholarship (to G.M.).

Conflicts of interest

None declared.

Data availability

The data underlying this article will be shared on reasonable request to the corresponding author.

References

1. Cahalan MD, Chandy KG. The functional network of ion channels in T lymphocytes. Immunol Rev. 2009;231:59–87. https://doi.org/10.1111/j.1600-065X.2009.00816.x
2. Feske S, Skolnik EY, Prakriya M. Ion channels and transporters in lymphocyte function and immunity. Nat Rev Immunol. 2012;12:532–547. https://doi.org/10.1038/nri3233

3. Chirra M et al. How the potassium channel response of T lymphocytes to the tumor microenvironment shapes antitumor immunity. Cancers (Basel) 2022;14:3564. https://doi.org/10.3390/cancers14153564
4. Wulff H et al. The voltage-gated Kv1.3 K+ channel in effector memory T cells as new target for MS. J Clin Invest. 2003;111:1703–1713. https://doi.org/10.1172/JCI16921
5. Ghanshani S et al. Up-regulation of the IKCa1 potassium channel during T-cell activation. J Biol Chem. 2000;275:37137–37149. https://doi.org/10.1074/jbc.M003941200
6. Schwarz EC, Qu B, Hoth M. Calcium, cancer and killing: the role of calcium in killing cancer cells by cytotoxic T lymphocytes and natural killer cells. Biochim Biophys Acta. 2013;1833:1603–1611. https://doi.org/10.1016/j.bbamcr.2012.11.016
7. Koshy S et al. Blocking KCa3.1 channels increases tumor cell killing by a subpopulation of human natural killer lymphocytes. PLoS One. 2013;8:e76740. https://doi.org/10.1371/journal.pone.0076740
8. Eil R et al. Ionic immune suppression within the tumour microenvironment limits T cell effector function. Nature. 2016;537:539–543. https://doi.org/10.1038/nature19364
9. Gurusamy D, Clever D, Eil R, Restifo NP. Novel 'elements' of immune suppression within the tumor microenvironment. Cancer Immunol Res. 2017;5:426–433. https://doi.org/10.1158/2326-6066.CIR-17-0117
10. Benmebarek M-R et al. Killing mechanisms of chimeric antigen receptor (CAR) T cells. Int J Mol Sci. 2019;20:1283. https://doi.org/10.3390/ijms20061283
11. Denlinger N, Bond D, Jaglowski S. CAR T-cell therapy for B-cell lymphoma. Curr Probl Cancer. 2022;46:100826. https://doi.org/10.1016/j.currproblcancer.2021.100826
12. Li J et al. Chimeric antigen receptor T cell (CAR-T) immunotherapy for solid tumors: lessons learned and strategies for moving forward. J Hematol Oncol. 2018;11:22. https://doi.org/10.1186/s13045-018-0568-6
13. Hanahan D, Coussens LM. Accessories to the crime: functions of cells recruited to the tumor microenvironment. Cancer Cell. 2012;21:309–322. https://doi.org/10.1016/j.ccr.2012.02.022
14. Chimote AA et al. A defect in KCa3.1 channel activity limits the ability of $CD8^+$ T cells from cancer patients to infiltrate an adenosine-rich microenvironment. Sci Signal. 2018;11:eaaq1616. https://doi.org/10.1126/scisignal.aaq1616
15. Dong R et al. Rewired signaling network in T cells expressing the chimeric antigen receptor (CAR). EMBO J. 2020;39:e104730. https://doi.org/10.15252/embj.2020104730
16. Voros O, Panyi G, Hajdu P. Immune synapse residency of Orai1 alters $Ca2^+$ response of T cells. Int J Mol Sci. 2021;22:11514. https://doi.org/10.3390/ijms222111514
17. Kummerow C et al. A simple, economic, time-resolved killing assay. Eur J Immunol. 2014;44:1870–1872. https://doi.org/10.1002/eji.201444518
18. Fleig A, Parekh AB. New insights into Ca^{2+} channel function in health and disease. J Physiol. 2017;595:2997–2998. https://doi.org/10.1113/JP274289
19. Capera J et al. Dynamics and spatial organization of Kv1.3 at the immunological synapse of human $CD4^+$ T cells. Biophys J. 2024;123:2271–2281. https://doi.org/10.1016/j.bpj.2023.08.011
20. Nicolaou SA et al. Localization of Kv1.3 channels in the immunological synapse modulates the calcium response to antigen stimulation in T lymphocytes. J Immunol. 2009;183:6296–6302. https://doi.org/10.4049/jimmunol.0900613
21. Medyouni G et al. Inhibition of K+ channels affects the target cell killing potential of CAR T cells. Cancers (Basel). 2024;16:3750. https://doi.org/10.3390/cancers16223750
22. Nicolaou SA et al. Differential calcium signaling and Kv1.3 trafficking to the immunological synapse in systemic lupus erythematosus. Cell Calcium. 2010;47:19–28. https://doi.org/10.1016/j.ceca.2009.11.001
23. Zhang Y et al. Exploring CAR-T cell therapy side effects: mechanisms and management strategies. J Clin Med. 2023;12:6124. https://doi.org/10.3390/jcm12196124
24. Tang T, Jian B, Liu Z. Transmembrane protein 175, a lysosomal ion channel related to Parkinson's disease. Biomolecules. 2023;13:802. https://doi.org/10.3390/biom13050802
25. Ren YR et al. Clofazimine inhibits human Kv1.3 potassium channel by perturbing calcium oscillation in T lymphocytes. PLoS One. 2008;3:e4009. https://doi.org/10.1371/journal.pone.0004009
26. Bloemberg D et al. A high-throughput method for characterizing novel chimeric antigen receptors in Jurkat cells. Mol Ther Methods Clin Dev. 2020;16:238–254. https://doi.org/10.1016/j.omtm.2020.01.012
27. Panyi G, Vámosi G, Bodnár A, Gáspár R, Damjanovich S. Looking through ion channels: recharged concepts in T-cell signaling. Trends Immunol. 2004;25:565–569. https://doi.org/10.1016/j.it.2004.09.002
28. Srivastava S et al. The class II phosphatidylinositol 3 kinase C2beta is required for the activation of the K^+ channel KCa3.1 and CD4 T-cells. Mol Biol Cell. 2009;20:3783–3791.
29. Chiang EY et al. Potassium channels Kv1.3 and KCa3.1 cooperatively and compensatorily regulate antigen-specific memory T cell functions. Nat Commun. 2017;8:14644. https://doi.org/10.1038/ncomms14644
30. Wu L et al. Targeting CAR to the peptide-MHC complex reveals distinct signaling compared to that of TCR in a Jurkat T cell model. Cancers (Basel). 2021;13:867. https://doi.org/10.3390/cancers13040867
31. Barden M et al. CAR and TCR form individual signaling synapses and do not cross-activate, however, can co-operate in T cell activation. Front Immunol. 2023;14:1110482. https://doi.org/10.3389/fimmu.2023.1110482

The Journal of Immunology, 2025, 214, 2796–2805
https://doi.org/10.1093/jimmun/vkaf199
Research Article